The contribution of cMyBP-C Ser282 phosphorylation to the rate of force generation and *in vivo* cardiac contractility

Kenneth S. Gresham[1], Ranganath Mamidi[1], and Julian E. Stelzer[1]

[1]Department of Physiology and Biophysics, School of Medicine, Case Western Reserve University, Cleveland, OH 44106, USA

Running title: Ser 282 Phosphorylation and Contractile Function

Key words: cMyBP-C phosphorylation, contractile function, cross-bridge kinetics

Word count excluding references and figure legends: 9,181

Table of Contents category:

Address for correspondence:

Julian E. Stelzer, Ph.D.

2109 Adelbert Rd, Robbins E522

Department of Physiology and Biophysics

School of Medicine, Case Western Reserve University

Cleveland, OH 44106

Phone: (216) 368-8636; Fax: (216) 368-5586

E-mail: julian.stelzer@case.edu

Key Points Summary

- Phosphorylation of cardiac myosin binding protein C (cMyBP-C) Ser282 has been proposed to modulate the phosphorylation of Ser273 and Ser302, and thereby the contractile response to increased β-adrenergic stimulation, yet the precise functional role of Ser282 is unknown.

- PKA phosphorylation of Ser273 and Ser302 was unaffected by Ser282 phospho-ablation, suggesting that Ser282 phosphorylation is not required for full phosphorylation of neighboring residues.

- Mice with Ser282 phospho-ablation (TG^{S282A}) displayed normal basal *in vivo* cardiac function but impaired rates of pressure development in response to β-adrenergic stimulation.

- Basal rates of cross-bridge kinetics were unaffected by Ser282 phospho-ablation, however, the PKA-mediated acceleration of cross-bridge recruitment was blunted in TG^{S282A} myocardium.

- Collectively, our data suggests that Ser282 phosphorylation is critical to achieve complete acceleration of cardiac contractile function in response to increased β-adrenergic stimulation, but also implicates Ser273 and Ser302 phosphorylation as important modulators of the cMyBP-C-mediated contractile response.

Word count: 150

ABSTRACT

Cardiac myosin binding protein-C (cMyBP-C) phosphorylation plays an important role in modulating cardiac muscle function and accelerating contraction. It has been proposed that Ser282 phosphorylation may serve as a critical molecular switch that regulates the phosphorylation of neighboring Ser273 and Ser302 residues, and thereby govern myofilament contractile acceleration in response to protein kinase A (PKA). Therefore, to determine the regulatory roles of Ser282 we generated a transgenic (TG) mouse model expressing cMyBP-C with a non-phosphorylatable Ser282 (i.e., serine to alanine substitution, TG^{S282A}). Myofibrils isolated from TG^{S282A} hearts displayed robust PKA-mediated phosphorylation of Ser273 and Ser302, and the increase in phosphorylation was identical to

TG type (TG^{WT}) controls. No signs of pathological cardiac hypertrophy were detected in TG^{S282A} hearts by either histological examination of cardiac sections or echocardiography. Baseline fractional shortening (FS), ejection fraction (EF), isovolumic relaxation time (IVRT), the rate of pressure development, and the rate of relaxation (τ) were unaltered in TG^{S282A} mice. However, the increase in cardiac contractility as well as the acceleration of pressure development observed in response to β-adrenergic stimulation was attenuated in TG^{S282A} mice. In agreement with our *in vivo* data, *in vitro* force measurements revealed that PKA-mediated acceleration of cross-bridge kinetics in TG^{S282A} myocardium was significantly attenuated compared to TG^{WT} myocardium. Taken together, our data suggests that while Ser282 phosphorylation does not regulate the phosphorylation of neighboring Ser residues and basal cardiac function, but full acceleration of cross-bridge kinetics and left ventricular pressure development cannot be achieved in its absence.

Abbreviations: cMyBP-C, cardiac myosin binding protein C; DOB, dobutamine; dp/dt, rate of LV pressure development; dp/dt_{max}, peak rate of left ventricular pressure development; EDP, end-diastolic pressure; EF, ejection fraction; ESP, end-systolic pressure; F_{max}, maximum Ca^{2+} activated force; F_{min}, Ca^{2+} independent force; FS, fractional shortening; H&E, hematoxylin and eosin stain; HR, heart rate; HSC70, heat shock chaperone 70; IVRT, isovolumic relaxation time; k_{df}, rate constant of delayed force development; k_{rel}, rate constant of force decay; k_{tr}, rate constant of force redevelopment; LV, left ventricle; n_H, Hill coefficient; NTG, non-transgenic; pCa_{50}, $[Ca^{2+}]$ required for 50%-maximum activation; PKA, protein kinase A; P, submaximal force; P_o, maximal force; P-V, pressure-volume; SL, sarcomere length; τ, rate constant of pressure relaxation; TG, transgenic; TG^{S282A}, mice expressing transgenic cMyBP-C with a serine to alanine mutation at residue 282; TG^{WT}, mice expressing transgenic WT cMyBP-C; TnI, troponin I; TnT, troponin T; XB, cross-bridge.

Introduction

In order to meet constantly changing systemic demand, the heart must modulate its output on a beat-to-beat basis. Increased cardiac output is achieved via increased β-adrenergic stimulation, which results in enhanced protein kinase A (PKA)-mediated phosphorylation of several key cardiac proteins. The principal targets of β-adrenergic signaling at the level of the myofilament are troponin I (TnI) and cardiac myosin binding protein-C (cMyBP-C) (Hartzell & Titus, 1982; Garvey *et al*. 1988), which together contribute to accelerated rates of contraction and relaxation at the myocyte level, and accelerated left-ventricular pressure development and relaxation at the whole heart level (Layland *et al*. 2005; Barefield & Sadayappan, 2010).

cMyBP-C, which is highly phosphorylated under basal conditions, becomes increasingly dephosphorylated in patients with hypertrophic cardiomyopathy and heart failure (Jacques *et al*. 2008; Copeland *et al*. 2010; El-Armouche *et al*. 2007), suggesting that phosphorylation of cMyBP-C is critical for normal cardiac function. In agreement, transgenic (TG) mouse models that express cMyBP-C with non-phosphorylatable serine residues 273, 282, and 302 (i.e., serine to alanine substitutions at Ser 273, 282, and 302) develop pathological cardiac hypertrophy and dysfunction and display a reduced contractile reserve in response to β-adrenergic stimulation (Sadayappan *et al*. 2005; Tong *et al*. 2008). Although it appears that there are other cMyBP-C residues which can be substrates for kinase activity (Copeland *et al*. 2010; Jia et al., 2010; Kuster *et al*. 2013), Ser273, 282, and 302 have been shown to be critical in modulating cardiac function in both health and disease (Nagayama *et al*. 2007; Tong *et al*. 2008).

Phosphorylation of cMyBP-C by PKA has been proposed to relieve a constraint on the myosin heads that allows increased interaction between myosin and the thin filament (Gruen *et al*. 1999, Colson *et al*. 2008 & 2012). cMyBP-C phosphorylation accelerates the rate of force redevelopment, a measure of cross-bridge (XB) cycling kinetics, at submaximal Ca^{2+} activation (Stelzer *et al*. 2006b; Stelzer *et al*. 2007), the activation range in which force generation is highly dependent on cooperative recruitment of XBs which progressively activate neighboring thin filament subunits (reviewed by Moss *et al*. 2004). Previous investigations of the regulatory roles of PKA-mediated cMyBP-C phosphorylation on cardiac muscle contraction have been performed by site-directed mutagenesis of all three of phosphorylatable serine residues (273, 282, and 302, i.e., TG3SA) (Tong *et al*. 2008; Colson *et al*. 2012) and have shown that preventing cMyBP-C phosphorylation by PKA eliminates

the acceleration of XB kinetics. However, the contribution of each of the individual Ser residues in the contractile response to PKA phosphorylation and how each site contributes to the *in vivo* response to β-adrenergic stimulation remains largely unknown. In this regard, earlier work suggested that there was a hierarchical phosphorylation pattern in which Ser282 phosphorylation was permissive for the phosphorylation of the remaining serine residues (Gautel *et al*. 1995). When Ser282 was mutated to an alanine residue (ablating phosphorylation at Ser282) and incubated with PKA, phosphorylation of the remaining phosphorylatable serine residues was decreased to 9% of wild-type (WT) levels (Gautel *et al*. 1995). An analysis of the time course of PKA-induced phosphorylation revealed that cMyBP-C was initially phosphorylated at one site, presumably at Ser282, with full phosphorylation of all three sites occurring only at a later time point (Gruen *et al*. 1999). A more recent study has also supported the idea that Ser282 phosphorylation is required for phosphorylation of the other remaining serine residues *in vitro* (Sadayappan *et al*. 2011). Wang *et al*. 2014 presented evidence that non-phosphorylatable Ser282, when coupled with phosphomimetic Ser273 and Ser302 residues, impairs cardiac contractile function by negatively impacting tension development and altering XB kinetics, suggesting that Ser282 could be critical in mediating the accelerating effects of PKA on XB kinetics (Wang *et al*. 2014). To date, however, no study has been conducted to examine the role of individual Ser residues in the PKA-mediated acceleration of XB kinetics, a fact that limits our understanding of cMyBP-C's phosphorylation-dependent regulation of contraction.

Therefore, the goals of this study were to determine if Ser282 phosphorylation is critical for the cMyBP-C-mediated regulatory response to PKA, to test whether Ser273 and Ser302 also contribute to changes in the rate of force generation in response to PKA, and to establish if Ser282 phosphorylation is critical for acceleration of *in vivo* cardiac function. To achieve these goals we have generated a TG mouse model that expresses a constitutively non-phosphorylatable cMyBP-C Ser282 by mutating the Ser282 to an alanine residue (S282A), and we investigated the effects of S282A on *in vitro* and *in vivo* cardiac contractile function, prior to and following PKA and dobutamine treatments, respectively.

Materials and methods

Ethical approval and generation of mouse models: This study was conducted in accordance with the *Guide for the Care and Use of Laboratory Animals* (NIH Publication No. 85-23, Revised 1996), and the procedures for anesthesia, surgery, and general care of the animals were approved by the Institutional Animal Care and Use Committee at Case Western Reserve University. Mice of both sexes (aged 3-6 months) were used for all studies. TG mice expressing cMyBP-C with a serine to alanine substitution at residue 282 (TG^{S282A}) were generated on cMyBP-C$^{-/-}$ background (SV/129 strain) using procedures described previously (Tong *et al*. 2008). Mice expressing TG wild-type cMyBP-C (TG^{WT}) were previously generated and characterized (Tong *et al*. 2008). The cMyBP-C M-domain sequence containing Ser273, Ser282, and Ser302 is illustrated in Fig. 1 along with the TG S282A construct sequence. Non-transgenic (NTG) mice of the SV/129 strain were used as controls.

Histological analysis of cardiac tissue: Histological examination of hearts was carried out as described previously (Cheng *et al*. 2013). Mouse hearts were formalin fixed for 4 hrs and subsequently sectioned at their mid-left ventricles (LVs). Dissected hearts remained in formalin overnight, paraffin embedded, and sectioned at 5µm thickness using a microtome. Staining of the cross sections was done with hematoxylin and eosin (H&E) (Cheng *et al*. 2013).

In vivo cardiac morphology and hemodynamic function: Evaluation of overall cardiac morphology and *in vivo* cardiac function was performed by echocardiography on anesthetized mice (1.5-2.0% isoflurane) (n = 8 mice per group), using a Sequoia C256 system (Siemens Medical, Malvern, PA, USA), according to a protocol described previously (Cheng *et al*. 2013). Pressure-volume (PV) loop analysis was performed on anesthetized (1.5-2.0% isoflurane) and ventilated mice to asses LV contractile properties as previously described (Cheng *et al*. 2013). Ventricular pressure and heart rate (HR) were allowed to stabilize before recording baseline parameters, after which an intraperitoneal (i.p.) injection of dobutamine (10µg/g) was administered to measure the response to β-adrenergic stimulation. PV loop analysis was performed offline using LabChart7 software P-V Loop and Peak analysis modules (ADInstruments, Dunedin, New Zealand).

Preparation and PKA phosphorylation of myocardium for SDS gel and Western blot analysis: Cardiac myofibrils were isolated from frozen mouse hearts on the day of the experiment. A section of the frozen tissue was placed in a fresh relaxing solution, homogenized, and myofibrils were skinned for 15 minutes using 1% Triton X-100 (Cheng *et al*. 2013). Skinned myofibrils were resuspended in fresh relaxing solution containing protease and phosphatase inhibitors (PhosSTOP and cOmplete ULTRA Tablets; Roche Applied Science, Indianapolis, IN, USA) and were kept on ice until use. Myofibrils, PKA, and all solutions were brought to room temperature (22°C) before initiating the reaction. Myofibrils were incubated for 1 hr, at 30°C in a solution containing the catalytic subunit of bovine PKA (Tong *et al*. 2008) with the final concentration of PKA at 0.15U/µg myofibrils. Control myofibrils were incubated under the same conditions in the absence of PKA. To assess the effects of S282A phospho-ablation on the time course of PKA phosphorylation, myofibrils isolated from TG^{WT} and TG^{S282A} hearts were incubated in PKA for 15min, 30min, 45min, and 60min, and subsequently the levels of cMyBP-C phosphorylation were quantified. The PKA reactions were stopped by the addition of Laemmli buffer and samples were heated to 90°C for 5 mins and stored at -20°C until use for Western blots and Pro-Q analysis.

Western blot and Pro-Q analysis of myocardial samples: 10µg of the solubilized myofibrils were loaded and electrophoretically separated using 4-20% Tris-glycine gels (Lonza Walkersville Inc., Rockland, ME, USA) at 180V for 70 min. Western blots were performed as previously described (Cheng *et al*. 2013). PVDF membranes were incubated overnight with one of the following antibodies: total cMyBP-C (Santa Cruz Biotechnology, Santa Cruz, CA, USA), phospho-serine antibodies specific for Ser273, Ser282, or Ser302 phosphorylation (21st Century Biochemical, Marlborough, MA, USA; Cheng *et al*. 2013), myc tag (Santa Cruz Biotechnology), or heat shock cognate protein 70 (HSC70) (Santa Cruz Biotechnology). To determine the level of total protein phosphorylation, gels were fixed and stained with Pro-Q diamond phosphoprotein stain (Invitrogen, Carlsbad, CA, USA) and coomassie blue. Densitometric scanning of Western blots and stained gels was performed using Image J software (U.S. National Institutes of Health, Bethesda, MD, USA).

Myofilament Contractile Function

Solutions for experiments with skinned ventricular myocardium: Preparation of skinned ventricular myocardium was performed according to procedures described previously (Cheng *et al.* 2013). In brief, ventricular tissue was homogenized in a relax solution and skinned for 30 minutes using 1% Triton-X 100. A computer program (Fabiato, 1988) and known stability constants (Godt & Lindley, 1982) were used to calculate the composition of Ca^{2+} activation solutions. All solutions contained the following (in mM): 100 N, N-bis (2-hydroxyethyl)-2-aminoethanesulfonic acid (BES), 15 creatine phosphate, 5 dithiothreitol, 1 free Mg^{2+}, and 4 MgATP. The maximal activating solution (pCa 4.5; pCa = -log $[Ca^{2+}]_{free}$) also contained 7 EGTA and 7.01 $CaCl_2$; while the relaxing solution (pCa 9.0) contained 7 EGTA and 0.02 $CaCl_2$; and the pre-activating solution contained 0.07 EGTA. The pH of the Ca^{2+} solutions was adjusted to 7.0 with KOH (at 22°C) and the ionic strength was 180 mM. A range of pCa solutions, containing different amounts of $[Ca^{2+}]_{free}$, were made by mixing appropriate volumes of pCa 9.0 and 4.5 solutions.

Apparatus and experimental protocols: Skinned myocardial preparations were mounted in between a motor arm (312C; Aurora Scientific Inc., Aurora, Ontario, Canada) and a force transducer (403A; Aurora Scientific Inc.) as described previously (Cheng *et al.* 2013; Merkulov *et al.* 2012). Changes in the motor position and signals from the force transducer were sampled at 2.0 kHz using sarcomere length (SL) control software (Campbell & Moss, 2003). For all mechanical measurements, the SL of the muscle preparations was set to 2.1 μm and the experiments were performed at 22°C (Cheng *et al.* 2013; Merkulov *et al.* 2012).

Force-pCa Relationships: Force-pCa relationships were obtained and analyzed as described previously (Desjardins *et al.* 2012; Cheng *et al.* 2013). Submaximal force (P) developed at each pCa was normalized to maximal force (P_o, at pCa 4.5) i.e., P/P_o to construct the force-pCa relationships. The steepness of a Hill plot transformation of the force-pCa relationship was used to estimate the apparent cooperativity of force development. The force-pCa data were fit using the equation $P/P_o = [Ca^{2+}]^{nH}/(k^{nH} + [Ca^{2+}]^{nH})$, where n_H is the Hill coefficient and k is the $[Ca^{2+}]$ required to reach half-maximal activation (i.e., pCa_{50}).

Measurement of the rate of force redevelopment (k_{tr}): Measurement of k_{tr} in Ca^{2+}-activated muscle fibers was performed according to a mechanical slack-restretch maneuver described previously (Stelzer *et al*. 2006a; Chen *et al*. 2010; Cheng *et al*. 2013). k_{tr} was measured to assess the rate of XB transitions from weak- to strong-binding states (Brenner & Eisenberg, 1986; Campbell, 1997). Skinned preparations were transferred from relaxing (pCa 9.0) to an activating solution (pCa ranging from 6.2 to 4.5) and were allowed to develop a steady-state force. Once the muscle fiber achieved steady-state isometric force, it was rapidly slacked by 20% of its original muscle length which resulted in a rapid decline in force. After a brief period of unloaded shortening (10 ms), the preparation was rapidly restretched back to its original length and the time course of force redevelopment was measured. k_{tr} for each slack-restretch maneuver was estimated by linear transformation of the half-time of force redevelopment, i.e., $k_{tr} = 0.693/t_{1/2}$, as described previously (Chen *et al*. 2010; Cheng *et al*. 2013).

Stretch Activation Experiments: Stretch activation experiments were carried out as previously described (Cheng *et al*. 2013). Fibers were placed in pCa solutions that yielded submaximal force (~50% maximal force) and were allowed to develop a steady-state tension. Fibers were rapidly stretched by 2% of initial muscle length and held at the increased length for 5 seconds before being returned to relaxing solution. The stretch activation variables are shown in Fig X and the characteristic features of the stretch activation have been described previously (Stelzer *et al*. 2006c; Ford *et al*. 2010). In brief, a sudden 2% stretch of the muscle fiber produces in an instantaneous increase in force (P_1), which results from the strain of bound XBs. The strained XBs then rapidly detach, with a characteristic rate constant k_{rel}, and result in a rapid decline in force to reach minimum amplitude (P_2). Following this rapid decline, force develops gradually, with a characteristic rate constant k_{df}, as a result of length-induced recruitment of additional XBs into the force-producing state (Stelzer *et al*. 2006c) and reaches a new steady-state level (P_3). Stretch activation amplitudes were normalized to prestretch Ca^{2+}-activated force and were measured as described previously (Desjardins *et al*. 2012, Cheng *et al*. 2013). The time course of force decay was fit to a single exponential to yield k_{rel} and k_{df} was determined by a linear transformation of the half time of force redevelopment as previously described (Stelzer *et al*. 2006c).

Measurement of PKA-mediated effects on contractile function: For experiments assessing the functional effects of PKA phosphorylation on XB kinetics and force-pCa relationships, skinned preparations were incubated with the catalytic subunit of bovine PKA (Sigma-Aldrich, St. Louis, MO, USA), for 1 hr (at 22°C), in a pCa 9.0 solution (final concentration 0.25 U/μl) (Cheng *et al*. 2013). Experimental protocols following PKA treatment were repeated as described above.

Statistical analysis: Comparisons between groups was performed using a one-way analysis of variance (ANOVA) followed by Tukey-Kramer post hoc test, and comparisons of baseline and PKA or dobutamine treatments within groups was performed using a student's *t*-test as appropriate. All data are presented as means ± SEM. The criterion for statistical significance was set at $P < 0.05$.

RESULTS
Western blot and Pro-Q analysis of NTG and TG myofilament protein content and phosphorylation

To determine the relative expression of cMyBP-C in TG^{S282A} hearts, myocardial samples were electrophoretically separated on a 4-20% SDS gel and transferred onto a PVDF membrane for Western blot analysis (Fig. 1B). TG expression was confirmed by the presence of a myc-tag band in TG^{S282A} samples, which was absent in NTG samples. Densitometric scanning of the SDS gels (Fig. 1C) indicated that the expression of cMyBP-C with S282A in the hearts of TG^{S282A} mice was 85±3% when compared to the expression of cMyBP-C in the NTG hearts (Fig. 1D). The expression of cMyBP-C in TG^{WT} hearts was previously characterized as 72±3% of NTG control (Tong *et al*. 2008). The expression level of cardiac troponin I (TnI), another key sarcomeric protein, was not altered in TG^{S282A} hearts (Fig. 1D). Ser282 phospho-ablation in TG^{S282A} hearts was confirmed by Western blot using an antibody specific for phosphorylated Ser282 (Fig 1B), which showed a robust band in NTG samples that was absent in TG^{S282A} samples (Fig. 1B). Phosphorylation of Ser273 and Ser302 was detected in both NTG and TG^{S282A} samples (Fig 1B). HSC70 was used as a loading control to show that equal amounts of the samples have been loaded onto the gels (Fig. 1B).

Next, we assessed if abolishing phosphorylation of Ser282 prevents the PKA-mediated phosphorylation of neighboring phosphorylatable sites (Ser273 and Ser302) within the M-domain of cMyBP-C (Fig. 2). All phosphorylation values in TG^{S282A} myocardium were normalized to TG^{WT} phosphorylation levels after PKA treatment (Figs. 2A and 2B) to facilitate comparisons between the two groups. Densitometric analysis of Western blots (Fig. 2A) indicated that the basal phosphorylation of Ser273 was not significantly different between the groups ($47\pm4\%$, $54\pm8\%$, and $61\pm5\%$ for NTG, TG^{WT}, and TG^{S282A}, respectively) (Fig. 2B). The basal phosphorylation of Ser282 was also similar in NTG and TG^{WT} groups ($67\pm9\%$ and $74\pm11\%$ for NTG and TG^{WT}, respectively), but was absent in TG^{S282A} samples (Figs. 2A and 2B). Ser302 phosphorylation levels were low at baseline for all three groups, with phosphorylation of Ser302 in TG^{S282A} myofibrils being slightly elevated ($5\pm1\%$, $6\pm1\%$, and $11\pm1\%$ for NTG, TG^{WT}, and TG^{S282A}, respectively; $P<0.05$, Figs. 2A and 2B). To determine whether PKA-mediated Ser273 and Ser302 phosphorylation could still be achieved in the absence of Ser282 phosphorylation, myofibrils isolated from NTG, TG^{WT}, and TG^{S282A} hearts were incubated with PKA for 1 hr (see methods). Phosphorylation of both Ser273 ($102\pm5\%$, $100\pm12\%$, and $99\pm7\%$ for NTG, TG^{WT}, and TG^{S282A}, respectively) and Ser302 ($91\pm8\%$, $100\pm7\%$, and $94\pm3\%$ for NTG, TG^{WT}, and TG^{S282A}, respectively) increased with PKA treatment in TG^{S282A} samples, indicating that abolishing phosphorylation at Ser282 does not prevent PKA-mediated phosphorylation of Ser273 or Ser302 (Figs. 2A and 2B). PKA phosphorylation of Ser282 was similar in NTG and TG^{WT} groups ($106\pm11\%$ and $100\pm8\%$ for NTG and TG^{WT}, respectively) and was absent in TG^{S282A} samples. To determine if the rate of PKA-mediated cMyBP-C phosphorylation was altered by Ser282 phospho-ablation, TG^{WT} and TG^{S282A} myofibrils were treated with PKA for 15min, 30min, 45min, or 60min, and Ser273 and Ser302 phosphorylation was examined by Western Blot (Fig 2C). No differences in the rate of Ser273 and Ser302 phosphorylation were observed at any time point examined, demonstrating that the rate of PKA-mediated Ser273 and Ser282 phosphorylation was unaffected by Ser282 phospho-ablation.

We also assessed whether abolishing phosphorylation of Ser282 impacts the phosphorylation of other important regulatory sarcomeric proteins such as troponin T (TnT), TnI, and myosin regulatory light chain (RLC) (Figs. 2C and 2D). The relative protein phosphorylation values (phosphorylation signal/total protein signal) are presented in Fig. 2E. Our results indicate that the baseline phosphorylation of TnT and TnI was similar between all the groups: $62\pm6\%$, $64\pm6\%$, and $61\pm6\%$, for TnT and $66\pm6\%$, $73\pm0\%$, and $80\pm6\%$, for TnI in

11

NTG, TG^{WT}, and TGS^{282A} samples, respectively. Furthermore, PKA phosphorylation of TnT and TnI was unaffected by the presence of S282A substitution in cMyBP-C as increases in phosphorylation following PKA treatment were similar in all the groups (99±7%, 100±1%, and 107±4% for TnT and 102±9%, 100±2%, and 108±8%, for TnI in NTG, TG^{WT}, and TG^{S282A} samples, respectively). Phosphorylation of RLC was unaffected by PKA treatment and thus was similar between all the three groups under both basal and PKA-treated conditions.

Histological assessment of cardiac morphology

To examine if TG incorporation of cMyBP-C affects cardiac morphology, we examined histological sections of tissue prepared from NTG, TG^{WT}, and TG^{S282A} hearts that were stained with H&E. Representative cross sections for NTG, TG^{WT}, and TG^{S282A} hearts are presented in Fig. 3, along with representative formalin fixed hearts from each group. TG^{S282A} hearts exhibited similar overall size and morphology with no noticeable alterations in their chamber geometry when compared to control NTG and TG^{WT} sections (Fig. 3), indicating that TG expression of S282A cMyBP-C did not induce any overt cardiac pathology.

Echocardiography

Echocardiography was used to further confirm the effects of TG S282A expression on LV morphology and to test the impact of Ser282 phospho-ablation on *in vivo* LV function (Table 1). Cardiac morphology was assessed by LV mass (normalized to body weight) and posterior wall thickness in diastole and systole. TG^{S282A} hearts displayed no significant increase in heart weight or wall thickness, indicating an absence of pathological hypertrophy. Taken together, these results along with the observations from histological sections suggest that abolishing Ser282 phosphorylation does not affect overall cardiac morphology. Measures of systolic and diastolic function were evaluated to further assess the impact of Ser282 phosphorylation on cardiac performance. Ejection fraction (EF) and fractional shortening (FS), measures of the systolic function, were not different in TG^{S282A} hearts compared to TG^{WT} controls (Table 1). Additionally, the isovolumic relaxation time (IVRT), a measure of diastolic function, showed no differences between any of the groups (Table 1). These results indicate that Ser282 phospho-ablation had no significant impact on overall *in vivo* cardiac performance at baseline.

Hemodynamics

To assess the impact of Ser282 phospho-ablation on the contractile response to β-adrenergic stimulation, cardiac function was measured by P-V loop catheterization in response to dobutamine administration (Table 2). In agreement with echocardiography results, TG^{S282A} mice displayed no differences in baseline function as assessed by the peak rate of pressure development ($dp/dt_{max)}$ or τ, the relaxation time constant. In NTG and TG^{WT} hearts, dobutamine significantly accelerated dp/dt_{max} to a similar extent above baseline rates. Interestingly, in TG^{S282A} mice dp/dt_{max} was significantly accelerated from baseline by dobutamine, but the acceleration was significantly less than TG^{WT} values after dobutamine (Table 2), suggesting that ablation of Ser282 phosphorylation prevents full acceleration of pressure development in response to dobutamine administration. Post-dobutamine τ was similar in all groups. No differences in heart rate or end-systolic and diastolic pressure were observed between groups at baseline or after dobutamine administration.

To further characterize the impact of Ser282 phospho-ablation on the acceleration of pressure development in response to dobutamine, we assessed the rate of pressure change (dp/dt) over a range of developed pressures in the left ventricle prior to ejection (Fig 4A). End diastolic pressure (EDP) was subtracted from instantaneous ventricular pressure to calculate developed pressure (P_d) during isovolumic contraction before the onset of ejection. In all groups, dp/dt increased as pressure developed in the left ventricle until dp/dt reached a maximum around 40–50mmHg, at which point the rate of pressure development began to slow slightly until the onset of ejection. Dobutamine significantly accelerated dp/dt during pressure as indicated by an upward shift in the relationship between dp/dt and P_d (Fig. 4A). In TG^{S282A} hearts dobutamine significantly accelerated the rate of pressure development at every level of P_d examined; however, the acceleration of dp/dt was significantly less in TG^{S282A} hearts when compared to TG^{WT} hearts, reflected by a smaller upward shift in the dp/dt-P_d relationship (Fig 4A). The rate of pressure development at baseline was unaltered by phospho-ablation of Ser282, and the rate of pressure development in NTG hearts was not different when compared to TG^{WT} hearts at any ventricular pressure assessed, either at baseline or following dobutamine administration.

Additionally, we examined the time course of dp/dt to determine the role of Ser282 phosphorylation in accelerating early pressure development. Fig 4B shows the time taken to reach dp/dt_{max} (t_d) for TG^{WT} and TG^{S282A} hearts after the start of pressure development.

13

Baseline t_d was not different between the groups (11.4±0.6 ms and 12.0±0.4 ms for TG^{WT} and TG^{S282A}, respectively), and while dobutamine shortened the time to dp/dt$_{max}$ in both TG^{WT} and TG^{S282A}, TG^{S282A} mice reached dp/dt$_{max}$ significantly slower than TG^{WT} after dobutamine (8.4±0.4 ms and 9.8±0.4 ms for TG^{WT} and TG^{S282A}, respectively). The t_d in NTG hearts was not significantly different either at baseline or after dobutamine when compared to TG^{WT} hearts (data not shown). Heart rate had no effect on our observations, as TG^{S282A} t_d was still significantly slower when normalized to cardiac cycle duration (data not shown). We also examined the impact of TG S282A cMyBP-C expression on the time course of ventricular ejection (Fig 4C). Ejection time was similar between TG^{WT} and TG^{S282A} hearts at baseline, and dobutamine administration slightly shortened the duration of ejection to a similar extent in both groups (Fig 4C). No differences were detected between TG^{WT} and TG^{S282A} groups when ejection time was normalized to cardiac cycle duration either at baseline or following dobutamine infusion, demonstrating that ejection time is not impacted by the absence of Ser282 phosphorylation. This is in agreement with a previous study (Nagayama *et al*. 2007) which demonstrated that cMyBP-C plays a structural role in maintaining ejection that is independent of its phosphorylation status. Thus, these observations signify that the absence of a phosphorylatable Ser282 residue significantly alters the acceleration and timing of systolic pressure development following dobutamine administration. The t_d in NTG hearts was not significantly different either at baseline or after dobutamine when compared to TG^{WT} hearts. Taken together, our analysis of the rate of pressure development further demonstrates that baseline function can be maintained in the absence of Ser282 phosphorylation, and although cardiac contractility can be accelerated in the absence of Ser282 phosphorylation, pressure development in hearts lacking Ser282 phosphorylation cannot be accelerated to the same extent as in hearts that have 3 phosphorylatable Ser residues.

Measurement of steady-state mechanical properties

Steady-state force generation, cooperativity of force generation (n_H) and myofilament Ca^{2+} sensitivity of force generation (pCa$_{50}$) were measured to assess the effects of Ser282 phospho-ablation on myocardial mechanical properties. At baseline, there were no differences in Ca^{2+}-independent force (measured at pCa 9.0; F$_{min}$), maximum Ca^{2+}-activated force (measured at pCa 4.5; F$_{max}$), n_H, and pCa$_{50}$ between NTG, TG^{WT}, and TG^{S282A} (Table 3). Furthermore, the addition of PKA had no effect on the minimum or the maximum force produced and n_H in all the groups tested, in agreement with earlier findings (Cheng *et al*.

2013, Stelzer *et al*. 2007, Tong *et al*. 2008). PKA treatment led to a similar decrease in the pCa_{50} in all groups when compared to the corresponding non-PKA treated values (Table 3). Thus, our data indicate S282A expression in the myocardium does not alter myofilament steady-state force generation under basal conditions or in response to PKA treatment.

Measurement of the rate constant of force redevelopment (k_{tr})

We measured the effect of TG^{S282A} on the rate constant of transition of XBs from weak- to strong-bindings states (k_{tr}) (Brenner & Eisenberg, 1986; Campbell, 1997) using a release-restretch protocol (Stelzer *et al*. 2007; Chen *et al*. 2010). k_{tr} was measured at 50% of maximal Ca^{2+} activation before and after PKA treatment (Fig 5) to determine the role of Ser282 in accelerating submaximal cooperative recruitment of strongly bound XBs. At baseline, no differences in k_{tr} were detected in NTG, TG^{WT}, or TG^{S282A} fibers, suggesting that the absence of Ser282 phosphorylation does not negatively impact basal force redevelopment. Treatment with PKA significantly accelerated k_{tr} in NTG, TG^{WT}, and TG^{S282A} fibers from baseline values; however, the acceleration in k_{tr} observed in TG^{S282A} was significantly less than TG^{WT} controls. After PKA treatment, TG^{S282A} k_{tr} at 50% of maximal Ca^{2+} activation was 16% less than in TG^{WT} controls (9.8±0.4 vs 11.7±0.4, p <0.05). A representative k_{tr} trace of TG^{S282A} skinned myocardium prior to and following PKA treatment is shown in Fig 5B. NTG k_{tr} was not significantly different than TG^{WT} after PKA treatment. Collectively, our results from k_{tr} measurements indicate that while abolishing phosphorylation at Ser282 does not alter k_{tr} at baseline or prevent an acceleration of k_{tr} at 50% maximal Ca^{2+}-activation induced by PKA, a full acceleration of XB kinetics could not be achieved in the absence of Ser282 phosphorylation.

Stretch activation

The role of Ser282 phosphorylation on the PKA-mediated response to dynamic strain-sensitive XB behavior was assessed by stretch activation experiments. A rapid stretch of 2% of initial muscle length was imposed on NTG, TG^{WT}, and TG^{S282A} myocardium at 50% of maximal Ca^{2+} activation before and after PKA treatment. Fig 6 illustrates a typical response of TG^{S282A} skinned myocardium to PKA treatment. PKA treatment accelerated the rate of force decay (k_{rel}) and the rate of delayed force redevelopment (k_{df}) in TG^{S282A} myocardium, results that were qualitatively similar to the PKA-mediated changes in stretch activation in NTG and TG^{WT} myocardium observed in this study (Table 4) and in previous work (Tong *et*

15

al. 2008). However, the absolute magnitude of the acceleration in k_{df} was significantly less in TG^{S282A} myocardium compared to TG^{WT} myocardium, as demonstrated by the reduced k_{df} after PKA treatment (Table 4). No significant differences in krel between TG^{S282A} and TG^{WT} skinned myocardium were observed. The amplitudes of all stretch variables were normalized to prestretch isometric force to facilitate comparisons between groups (Stelzer *et al*. 2006b). The amplitude of the initial rise in force (P_1), which results from stretch-induced strain of attached XBs, was decreased by PKA treatment to a similar extent in all groups. PKA treatment also increased the amplitude of the rapid decline in force (P_2) due to accelerated force decay, but did not alter the magnitude of the steady-state force achieved after stretch (P_3) (Table X), an effect that was observed in all groups. The increased rate of XB detachment after PKA treatment that led to an increase in the amplitude of P_2 also resulted in an increased amplitude of P_{df}, which was unaffected by the phosphorylation status of Ser282. All amplitudes were normalized to prestretch isometric force. No differences in k_{tr}, k_{rel}, of the amplitudes of P_1, P_2, P_3, or P_{df} were observed at baseline between groups. Our measurements of PKA-mediated acceleration of XB kinetics after a rapid stretch further demonstrate that while baseline kinetics can be maintained in the absence of Ser282 phosphorylation, the complete PKA-mediated acceleration of XB recruitment was not achieved in TG^{S282A} myocardium, indicating a role for Ser282 phosphorylation in the PKA-mediated acceleration of XB-induced cooperative activation of the thin filament.

DISCUSSION

Phosphorylation of Ser282 in cMyBP-C has been proposed to act as a molecular switch that dictates the phosphorylation of neighboring residues, Ser273 and Ser302 (Gautel *et al*. 1995); however, the functional effects of Ser282 phosphorylation and its role in modulating XB behavior are not fully understood. Thus, the purpose of this study was to determine the functional roles of Ser282 phosphorylation in the regulation of the contractile response to PKA treatment *in vitro*, and its role in modulating *in vivo* cardiac contractility in response to β-agonist stimulation. To delineate the functional effects of Ser282 phosphorylation on myofilament and whole heart function, we generated a TG mouse model (TG^{S282A}) expressing cMyBP-C with a non-phosphorylatable Ser282 (i.e., an alanine substitution for serine at position 282, S282A). Our results show that phospho-ablation of Ser282 does not prevent PKA-mediated phosphorylation of the neighboring M-domain phosphorylatable residues, Ser273 and Ser302. TG^{S282A} mice displayed normal cardiac

morphology and baseline contractile function as assessed by *in vivo* echocardiography and P-V loop analysis. Additionally, baseline steady-state force generation and dynamic XB kinetics as assessed by measurements of the rate constant of force redevelopment (k_{tr}) following a mechanical slack-restretch maneuver and the rates of XB relaxation (k_{rel}) and delayed force development (k_{df}) following a rapid acute mechanical stretch, were unaltered by Ser282 phospho-ablation. However, differences were observed in the ability of dobutamine *in vivo* and PKA *in vitro* to fully accelerate contractile kinetics in TG^{S282A}. While treatment of skinned myocardium with PKA or β-agonist infusion in live animals resulted in accelerated XB kinetics and rates of pressure development, respectively, the magnitude of acceleration was attenuated when Ser282 phosphorylation was blocked. Taken together, our results demonstrate that Ser282 phosphorylation does not regulate the phosphorylation status of Ser273 and Ser302, and that acceleration of pressure development and XB kinetics can be achieved in its absence, but full acceleration of contractility *in vitro* and *in vivo* most likely requires phosphorylation of all three M-domain Ser residues.

Effects of Ser282 phospho-ablation on Ser273 and Ser302 phosphorylation

Early experiments suggested that initial phosphorylation of Ser282 permits subsequent phosphorylation at neighboring serine residues, because bacterially derived recombinant cMyBP-C protein expressing serine to alanine substitutions at residue 282 nearly eliminated PKA-mediated phosphorylation of Ser273 and Ser302 (Gautel *et al*. 1995). This idea was later supported by experiments in both mutated recombinant cMyBP-C proteins and myofibrils isolated from TG mouse models expressing S282A cMyBP-C in the heart (Sadayappan *et al*. 2011), which showed decreased phosphorylation of Ser302 by PKA, PKC, and CamKII in the presence of a non-phosphorylatable Ser282 (i.e., S282A). It is not clear, however, why in Gautel *et al.* (Gautel *et al.,* 1995) phosphorylation of both Ser273 and Ser302 was severely blunted by S282A, whereas Sadayappan *et al*. (Sadayappan *et al.,* 2011) found only the phosphorylation of Ser302 is abolished in the presence of S282A. In contrast, there is also evidence that phosphorylation of Ser273 and Ser302 could still be achieved in recombinant cMyBP-C proteins expressing a non-phosphorylatable Ser282 residue (i.e., S282A) (Bardswell *et al*. 2010; Cuello *et al*. 2011). A recent study (Bardswell *et al*. 2010) demonstrated that phosphorylation of Ser282 is not required for phosphorylation of other serine residues within the M-domain, as it was shown that PKD can selectively phosphorylate

17

Ser302 in recombinant cMyBP-C proteins expressing an S282A substitution. Similarly, Cuello *et al.* (Cuello *et al.* 2011) observed an increase in Ser273 and Ser302 phosphorylation following PKA treatment in recombinant cMyBP-C proteins expressing a S282A substitution, suggesting that phosphorylation at Ser273 and Ser302 is not necessarily predicated on the phosphorylation status of Ser282. In agreement with the latter studies, our present data show that abolishing Ser282 phosphorylation in the myocardium had minimal effects on the basal phosphorylation of Ser273 or Ser302 and did not affect PKA-mediated increases in phosphorylation of Ser273 and Ser302 (Fig. 2), indicating that Ser282 phosphorylation is not a prerequisite for PKA-mediated phosphorylation of neighboring serine residues.

The basis for the differences between studies showing the functional effects of Ser282 phosphorylation is not known, however, it is possible that variability in the recombinant proteins utilized, differences in the experimental protocols of kinase phosphorylation assays, and variations in the TG mouse models utilized may have contributed to the observed discrepancies in the results reported. For example, purified rabbit cMyBP-C was used by Gautel *et al.* (Gautel *et al.* 1995) and recombinant His-tagged human cMyBP-C C1C2 fragments were used by Bardswell *et al.* and Cuello *et al.* (Bardswell *et al.* 2010; Cuello *et al.* 2011). Furthermore, differences in the experimental conditions of the PKA phosphorylation assays between studies such as the source of the kinase, the concentration of PKA utilized, and the length of PKA incubation, could have contributed to the divergent effects on cMyBP-C phosphorylation. There are also differences between the mouse models utilized in previous studies and the present study as the expression of TG S282A cMyBP-C in the hearts of mice employed in Sadayappan *et al.* (Sadayappan *et al.* 2011) was ~25-45%, whereas in this study cardiac expression of TG S282A cMyBP-C was ~85%. Additionally, minor differences in genetic background of the mice employed in different studies could underlie subtle observed differences in phosphorylation of cMyBP-C Ser residues (Tong *et al.,* 2008, Tong *et al.,* 2014), and any resulting functional differences.

Functional role of Ser282 phosphorylation in modulating XB kinetics

We studied the impact of TG expression of cMyBP-C with constitutively non-phosphorylatable Ser282 (S282A) on XB turnover kinetics by measuring k_{tr}, the rate constant of force redevelopment following a mechanical release-restretch maneuver (Brenner & Eisenberg, 1988). k_{tr} is the sum of the forward (f) and reverse (g) rate constants of the

transition of XBs from weak, non-force-bearing state to a strong, force-bearing state (Brenner & Eisenberg, 1986; Campbell, 1997) and can be used as an index of XB turnover kinetics in the myocardium. At low levels of Ca^{2+} activation force development in cardiac muscle is highly dependent on XB-mediated cooperative activation where initial strong-binding of XBs to actin cooperatively recruits additional XBs into strongly-bound states, thereby further activating the thin filament. XB-induced cooperative recruitment of additional XBs tends to slow the overall rate of force development at low levels of Ca^{2+} activation (Campbell, 1997), whereas at high levels of Ca^{2+} activation the transition of XBs into the strongly-bound state is less reliant on XB-mediated cooperativity, as more thin filament regulatory units are directly activated by the binding of Ca^{2+} to TnC. An acceleration of k_{tr} in skinned myocardium following PKA treatment is not a universal finding as some studies showed no change in XB turnover kinetics following PKA treatment (Hofmann & Lange, 1994; Janssen & de Tombe, 1997; Walker *et al*. 2011), and some other studies showed a decrease in XB turnover kinetics following PKA treatment (Hanft & McDonald 2009; Hanft & McDonald 2010). However, in agreement with previous studies from our laboratory, and others (Cheng *et al*. 2013, Stelzer *et al*. 2006b; Chen *et al*. 2010; Bardswell *et al*. 2010; Cuello *et al*. 2011), here we show that PKA treatment of WT skinned myocardium significantly accelerated k_{tr} at 50% of maximal Ca^{2+} activation when compared to the non-treated preparations (Fig. 5). The disparities in the reported effects of PKA phosphorylation on k_{tr} are unclear; however, they may be attributed to differences in the myocardial preparations, the temperature at which the k_{tr} measurements were assessed, and the concentrations of the PKA used for incubating the cardiac preparations. For example, Hanft & McDonald (Hanft & McDonald 2009; Hanft & McDonald 2010) used single myocytes, conducted the experiments at 13°C, and incubated their preparations with 0.125 U/μL of PKA for 45 minutes. On the other hand, in the present study we used multicellular myocardial preparations, performed the k_{tr} measurements at 22°C, and incubated our preparations with 0.250 U/μL of PKA for 1 hr. In the physiological context, slowed k_{tr} following PKA treatment (Hanft & McDonald 2010) has been interpreted to result from enhanced cooperative activation of the thin filaments which would progressively enhance the number of force-producing XBs working against a constant afterload resulting in faster loaded shortening, and therefore, enhanced systolic ejection and increased stroke volume (McDonald *et al*. 2012). In contrast, results from the present study are consistent with the idea that PKA treatment accelerates k_{tr} due to acceleration in the rate of cooperative activation of the thin filament and transitions of XBs into the force-producing

19

state, which results in faster pressure development during isovolumic contraction, thereby leaving more time for systolic ejection *in vivo,* which enhances stroke volume and cardiac output.

Our results show that basal k_{tr} at 50% maximal Ca^{2+} activation was not different between TG^{S282A} skinned myocardium and TG^{WT} skinned myocardium (Fig 5), demonstrating that basal XB kinetics were not affected by Ser282 phospho-ablation. Basal k_{tr} values were also not significantly different between TG^{S282A} and TG^{WT} myocardium at all levels of Ca^{2+}-activation (data not shown). Following PKA treatment, k_{tr} in TG^{S282A} skinned myocardium was significantly accelerated compared to baseline; however, the acceleration in k_{tr} was modestly (16%) but significantly less compared to TG^{WT} skinned myocardium (Fig 5), suggesting that a complete PKA-mediated acceleration of k_{tr} requires Ser282 phosphorylation.

We further investigated the functional effects of Ser282 phospho-ablation in the myocardium on dynamic strain-dependent XB behavior using a stretch activation mechanical perturbation in which a small stretch (2% of initial muscle length) is applied to an otherwise isometrically contracting muscle fiber (Stelzer *et al*. 2006c). The initial rise in force due to acute stretch (i.e., P_1) is related to the strain of strongly-bound XB's, and can be indicative of XB stiffness (Cheng *et al*. 2013). Following PKA treatment P_1 values were decreased in all groups (Table 4) despite similar levels of pre-stretch steady-state force prior to and following PKA treatment, suggesting that PKA phosphorylation reduced XB stiffness. Furthermore, PKA phosphorylation resulted in greater XB detachment as displayed by the decline in the amplitude (i.e., P_2) and rate of force relaxation (i.e, k_{rel}) following acute stretch (Table 4), which is also consistent with an increase in XB compliance in response to increased strain. These results are consistent with previous studies showing that cMyBP-C and its phosphorylation are important for modulation of radial and longitudinal stiffness in the sarcomere (Palmer *et al*. 2011, Cheng *et al*. 2013).

Phospho-ablation of Ser282 did not affect the amplitudes of P_1, P_2, or the acceleration of k_{rel} following PKA treatment (Table 4); however, TG^{S282A} skinned myocardium displayed a reduced acceleration in stretch-induced delayed XB recruitment (i.e., k_{df}) compared to TG^{WT} skinned myocardium (Table 4). This would suggest that the attenuation of PKA-mediated acceleration in TG^{S282A} skinned myocardium is likely due to impaired XB recruitment and transitions to force generating states resulting in an overall slowing of the stretch activation response (Stelzer *et al*. 2007). The diminished acceleration of k_{df} in

20

TG^{S282A} skinned myocardium in response to PKA treatment compared to TG^{WT} skinned myocardium nearly mirrored the differences observed in k_{tr} measurements between the two groups suggesting that slower k_{tr} in PKA treated TG^{S282A} skinned myocardium was likely due to incomplete acceleration of XB recruitment and transition to force-generating states (the forward rate constant, f) rather than changes in the rate of XB detachment (the reverse rate constant, g). Our results suggest that because Ser282 phosphorylation does not modulate the phosphorylation of Ser273 and Ser302, phosphorylation of these residues can accelerate XB kinetics independent of Ser282 phosphorylation. In agreement, Bardswell *et al.* (2010) reported that phosphorylation of Ser302 by PKD (which does not phosphorylate Ser273 or Ser282) can significantly accelerate XB kinetics at 50% maximal activation. If phosphorylation of each site can contribute to the modulation of XB kinetics, increasing phosphorylation levels at any of these three residues may be sufficient to accelerate XB kinetics above basal levels. Our finding that XB kinetics can be accelerated in the absence of Ser282 phosphorylation does not mean that Ser282 is not functionally important. In agreement with previous studies (Wang *et al.* 2014) we did not observe differences in basal XB kinetics between TG^{S282A} and TG^{WT} skinned myocardium, however, Ser282 phospho-ablation diminished the acceleration of XB kinetics in response to PKA treatment. Although the contribution of Ser282 to this response was modest, because force generation in cardiac muscle is a highly cooperative process, even a relatively small decrease in the rate of XB recruitment in response to PKA phosphorylation can significantly amplify the functional response to increased β-adrenergic stimulation *in vivo*. The functional significance of cMyBP-C residue-specific modulation of cardiac muscle contraction is unclear, but may be important in conditions of heart failure where a down-regulation of β-adrenergic signaling may result in increased activation of non-PKA kinases (Bardswell *et al.* 2012) which can target individual cMyBP-C residues, thereby providing an alternate mechanism for regulating myofilament function in response to acute sympathetic activation.

In vivo consequences of Ser282 phospho-ablation

The importance of cMyBP-C phosphorylation for normal *in vivo* cardiac function is underscored by studies employing animal models in which all three phosphorylatable serine residues were mutated to alanine residues (i.e., TG^{3SA}), which show impaired systolic and diastolic cardiac function coupled with compensatory hypertrophy (Sadayappan *et al.* 2005; Tong *et al.* 2008). Furthermore, cardiac hemodynamic assessment in mice expressing non-

phosphorylatable cMyBP-C revealed that cMyBP-C phosphorylation is critical for systolic preload dependent early pressure rise and rate-dependent and adrenergic contractile reserve in response to dobutamine administration (Nagayama *et al*. 2007). In this study, TG^{S282A} hearts did not display noticeable hypertrophy, as left-ventricular mass and wall thickness were not different from NTG and TG^{WT} hearts (Table 1). The lack of pathological hypertrophy was further confirmed by examination of formalin fixed hearts and cardiac sections stained with H&E that revealed no alteration in wall size or overall morphology. Additionally, no significant differences were observed in basal cardiac contractile function as assessed by echocardiography (EF and FS), and pressure-volume catheterization (maximal pressure development, dp/dt_{max}, or ventricular relaxation, τ) in TG^{S282A} mice when compared to NTG and TG^{WT} mice (Table 2). This is consistent with a previous report in which a similar model of Ser282 phospho-ablation did not result in altered basal systolic function or result in increased HW/BW ratios, although that study reported an increase in wall thickness (Sadayappan *et al*. 2011).

The rate of early (isovolumic) contraction is dependent on the rate of thin filament activation by both Ca^{2+} and strongly bound XBs (reviewed in Hanft *et al.* 2008) such that an impaired XB recruitment can significantly impact the magnitude and rate of pressure development *in vivo*. Dobutamine accelerates the maximum rate of early pressure development (dp/dt_{max}, Table 2) in part by increasing the rate of XB-induced cooperative activation of the thin filament through phosphorylation of cMyBP-C (Nagayama *et al*. 2007). In this study we observed an increase in dp/dt_{max} compared to baseline values after dobutamine administration in all of the groups; however, dp/dt_{max} was significantly slower in TG^{S282A} hearts compared to TG^{WT} controls (Table 1) after dobutamine, consistent with the *in vitro* attenuation of accelerated XB recruitment in TG^{S282A} myocardium. The attenuation of accelerated pressure development in TG^{S282A} was observed not only as a slower dp/dt_{max} but was also evident as a slower submaximal dp/dt, as demonstrated by plotting the rate of pressure development over various levels of developed pressure before ejection (Fig 4A). In both TG^{WT} and TG^{S282A} animals dobutamine administration significantly influenced the relationship between dp/dt and developed pressure as demonstrated by an upward shift of the curve, reflecting an increase in the contractile state of the myocardium (Fig 4); however, the shift was blunted in TG^{S282A} hearts compared to WT controls (Fig 4) reflecting an impaired enhancement of pressure development after dobutamine due to Ser282 phospho-ablation. Changes in end diastolic pressure (EDP) can have modest effects on the relationship between

22

dp/dt and developed pressure (an increase in preload will enhance the rate of pressure development) (Mason *et al*. 1971), but this most likely did not influence our results as TG^{S282A} and TG^{WT} hearts had no differences in EDP under similar conditions. The finding that Ser282 phosphorylation modulates the rate of early pressure development is consistent with previous findings (Nagayama *et al*. 2007) highlighting the importance of cMyBP-C phosphorylation-mediated regulation of cooperative XB activation of the thin filament to accelerating pressure development during isovolumic contraction in response to dobutamine. The acceleration in pressure development after dobutamine administration results in dp/dt_{max} being reached sooner when compared to baseline, consistent with an overall shortening of the cardiac cycle. By measuring the time to dp/dt_{max} (t_d), a measure of the contractile state of the myocardium independent of preload (Adler *et al*. 1996a & 1996b), we were able to assess whether Ser282 phospho-ablation would prolong the length of time required to reach dp/dt_{max} in TG^{S282A} animals. At baseline there were no differences in t_d between TG^{WT} and TG^{S282A} hearts (Fig 4B). After dobutamine administration, t_d was significantly shorter in both the TG^{S282A} and TG^{WT} hearts; however, the reduction in t_d was blunted in TG^{S282A} hearts compared to TG^{WT} hearts (i.e., t_d was significantly prolonged in TG^{S282A}). The differences in t_d between TG^{WT} and TG^{S282A} hearts were not due to differences in HR as there were no differences between groups either at baseline or following dobutamine infusion, and t_d was still significantly slower in TG^{S282A} compared to TG^{WT} post dobutamine when normalized to cardiac cycle duration (data not shown). Our results suggest that having two functional phosphorylation residues may be sufficient to maintain cardiac function under normal conditions, however, in conditions of increased cardiac workload (such as with increased β-adrenergic stimulation), all three phosphorylated sites may be required to fully accelerate pressure development. In agreement with this idea, other studies show that mutating more than one serine residue, whether to mimic phospho-ablation or pseudo-phosphorylation, can result in cardiac contractile dysfunction and maladaptive remodeling (Sadayappan *et al*. 2005; Tong *et al*. 2008; Sadayappan *et al*. 2011; Gupta *et al*. 2013).

Potential molecular and structural implications of Ser282 phosphorylation

The molecular basis for the PKA-mediated acceleration of XB kinetics in cardiac muscle is related to the phosphorylation dependent reversible interactions of cMyBP-C with both myosin S2 and actin. In the non-phosphorylated state, the cMyBP-C's N-terminal C0-C2 domains interact with myosin S2 and actin (Gruen *et al*. 1999; Shaffer *et al*. 2009) and

PKA phosphorylation of serines in the M-domain reduces these interactions (Gruen *et al*. 1999; Shaffer *et al*. 2009). Phosphorylation of cMyBP-C relieves the sterical constraint imposed by cMyBP-C on the myosin heads and accelerates XB interactions with actin (Gruen *et al*. 1999; Previs *et al*. 2012), in part due to an increase in the radial displacement of XBs towards actin which enhances the probability of actomyosin interactions (Colson *et al*. 2008 & 2012). Phosphorylation of cMyBP-C also reduces the binding affinity of cMyBP-C for actin (Shaffer *et al*. 2009) thereby reducing the inhibition on myofilament sliding velocity allowing for accelerated XB cycling (Shaffer *et al*. 2009; Weith *et al*. 2012; Coulton & Stelzer, 2012). Thus, through decreased binding and inhibition of cMyBP-C's interactions with myosin and actin, PKA-mediated phosphorylation of cMyBP-C provides a mechanism for accelerating XB kinetics in the myocardium. However, the role of phosphorylation of individual M-domain serine residues in the cMyBP-C-mediated regulation of actomyosin interaction is still not completely understood, and there is no definitive structural model that describes the M-domain. It has been proposed that Ser273 and Ser282 are in close proximity to each other on a β-strand of the Ig-like core of the M-domain directly opposite to a patch of negatively charged amino acids on the surface of myosin S2 (Ababou *et al*. 2008; Blankenfeldt *et al*. 2006) that is a part of the cMyBP-C-myosin S2 interaction interface, while Ser302 lies on the opposite side of the β-strand and in a loop that extends away from the Ig-like core region (Jeffries *et al*. 2008). It was proposed that introduction of negative charges due to phosphorylation of Ser273 and Ser282 which lie opposite to myosin S2 will repel this region away from myosin S2 and result in a structural rearrangement in the core region of M-domain, whereas subsequent phosphorylation of Ser302 may result in movement of the opposing loop region (Jeffries *et al*. 2008). Furthermore, another recent structural study employing NMR and modeling approaches predicted that phosphorylation of Ser273 primarily stabilizes and extends the helical structure of M-domain, whereas phosphorylation of Ser282 and Ser 302 has little effect on the M-domain's helical stability (Howarth *et al*. 2012), suggesting that phosphorylation of each site could have a disparate impact on the structural conformation of the M-domain. In the context of findings from our study, because phospho-ablation of Ser282 did not prevent the effects of PKA phosphorylation on XB kinetics (Table 4; Figs. 5 and 6), our results are consistent with structural models that predict that the effects of cMyBP-C phosphorylation on M-domain structure may be specific to the individual serine residue that is phosphorylated (Howarth *et al*. 2012), rather than a hierarchical model in which initial phosphorylation of Ser282 dictates structural

24

rearrangements that allow subsequent phosphorylation of other Ser residues (Gautel *et al*. 1995). Thus, based on previous results (Bardswell *et al*. 2010; Cuello *et al*. 2011) and data presented here, it is likely that each of the three individual M-domain serine phosphorylation residues are functionally important and capable of modulating contractile function independently of the phosphorylation status of neighboring serine residues.

COMPETING INTERESTS

There are no conflicts of interest.

AUTHOR CONTRIBUTION

All experiments were performed at the Department of Physiology and Biophysics, Case Western Reserve University, Cleveland, Ohio, USA. K.S.G., R.M., and J.E.S participated in performing the experiments and data collection. K.S.G. and J.E.S contributed to the conception and design of the experiments, and K.S.G., R.M., and J.E.S. contributed to the analysis and interpretation of data and in writing and revising the article. All authors approved the final version of the manuscript.

FUNDING

ACKNOWLEDGEMENTS

REFERENCES

Ababou A, Rostkova E, Mistry S, Le Masurier C, Gautel M & Pfuhl M (2008). Myosin binding protein C positioned to play a key role in regulation of muscle contraction: structure and interactions of domain C1. *J Mol Biol* **384,** 615–630.

Adler D, Monrad ES, Hess OM, Krayenbuehl HP & Sonnenblick EH (1996*a*). Time to dP/dt(max), a useful index for evaluation of contractility in the catheterization laboratory. *Clin Cardiol* **19,** 397–403.

Adler D, Nikolic SD, Sonnenblick EH & Yellin EL (1996*b*). Time to dP/dtmax, a preload-independent index of contractility: open-chest dog study. *Basic Res Cardiol* **91,** 94–100.

Bardswell SC, Cuello F, Kentish JC & Avkiran M (2012). cMyBP-C as a promiscuous substrate: phosphorylation by non-PKA kinases and its potential significance. *J Muscle Res Cell Motil* **33,** 53–60.

Bardswell SC, Cuello F, Rowland AJ, Sadayappan S, Robbins J, Gautel M, Walker JW, Kentish JC & Avkiran M (2010). Distinct sarcomeric substrates are responsible for protein kinase D-mediated regulation of cardiac myofilament Ca2+ sensitivity and cross-bridge cycling. *J Biol Chem* **285,** 5674–5682.

Barefield D & Sadayappan S (2010). Phosphorylation and function of cardiac myosin binding protein-C in health and disease. *J Mol Cell Cardiol* **48,** 866–875.

Blankenfeldt W, Thomä NH, Wray JS, Gautel M & Schlichting I (2006). Crystal structures of human cardiac beta-myosin II S2-Delta provide insight into the functional role of the S2 subfragment. *Proc Natl Acad Sci U S A* **103,** 17713–17717.

Brenner B & Eisenberg E (1986). Rate of force generation in muscle: correlation with actomyosin ATPase activity in solution. *Proc Natl Acad Sci U S A* **83,** 3542–3546.

Campbell K (1997). Rate constant of muscle force redevelopment reflects cooperative activation as well as cross-bridge kinetics. *Biophys J* **72,** 254–262.

Campbell KS & Moss RL (2003). SLControl: PC-based data acquisition and analysis for muscle mechanics. *Am J Physiol Heart Circ Physiol* **285,** H2857–2864.

Chen Y, Somji A, Yu X & Stelzer JE (2010). Altered in vivo left ventricular torsion and principal strains in hypothyroid rats. *Am J Physiol - Heart Circ Physiol* **299,** H1577–H1587.

Cheng Y-HF, Wan X, McElfresh TA, Chen X, Gresham KS, Rosenbaum DS, Chandler MP & Stelzer JE (2013). Impaired Contractile Function Due to Decreased Cardiac Myosin Binding Protein C Content in the Sarcomere. *Am J Physiol - Heart Circ Physiol* **305**, H52-65.

Colson BA, Bekyarova T, Locher MR, Fitzsimons DP, Irving TC & Moss RL (2008). Protein kinase A-mediated phosphorylation of cMyBP-C increases proximity of myosin heads to actin in resting myocardium. *Circ Res* **103,** 244–251.

Colson BA, Patel JR, Chen PP, Bekyarova T, Abdalla MI, Tong CW, Fitzsimons DP, Irving TC & Moss RL (2012). Myosin binding protein-C phosphorylation is the principal mediator of protein kinase A effects on thick filament structure in myocardium. *J Mol Cell Cardiol* **53,** 609–616.

Copeland O, Sadayappan S, Messer AE, Steinen GJM, van der Velden J & Marston SB (2010). Analysis of cardiac myosin binding protein-C phosphorylation in human heart muscle. *J Mol Cell Cardiol* **49,** 1003–1011.

Coulton AT & Stelzer JE (2012). Cardiac myosin binding protein C and its phosphorylation regulate multiple steps in the cross-bridge cycle of muscle contraction. *Biochemistry* **51,** 3292–3301.

Cuello F, Bardswell SC, Haworth RS, Ehler E, Sadayappan S, Kentish JC & Avkiran M (2011). Novel role for p90 ribosomal S6 kinase in the regulation of cardiac myofilament phosphorylation. *J Biol Chem* **286,** 5300–5310.

Desjardins CL, Chen Y, Coulton AT, Hoit BD, Yu X & Stelzer JE (2012). Cardiac myosin binding protein C insufficiency leads to early onset of mechanical dysfunction. *Circ Cardiovasc Imaging* **5,** 127–136.

El-Armouche A, Pohlmann L, Schlossarek S, Starbatty J, Yeh Y-H, Nattel S, Dobrev D, Eschenhagen T & Carrier L (2007). Decreased phosphorylation levels of cardiac myosin-binding protein-C in human and experimental heart failure. *J Mol Cell Cardiol* **43,** 223–229.

Fabiato A (1988). Computer programs for calculating total from specified free or free from specified total ionic concentrations in aqueous solutions containing multiple metals and ligands. *Methods Enzymol* **157,** 378–417.

Ford SJ, Chandra M, Mamidi R, Dong W & Campbell KB (2010). Model representation of the nonlinear step response in cardiac muscle. *J Gen Physiol* **136**, 159–177.

Garvey JL, Kranias EG & Solaro RJ (1988). Phosphorylation of C-protein, troponin I and phospholamban in isolated rabbit hearts. *Biochem J* **249,** 709–714.

Gautel M, Zuffardi O, Freiburg A & Labeit S (1995). Phosphorylation switches specific for the cardiac isoform of myosin binding protein-C: a modulator of cardiac contraction? *EMBO J* **14,** 1952–1960.

Godt RE & Lindley BD (1982). Influence of temperature upon contractile activation and isometric force production in mechanically skinned muscle fibers of the frog. *J Gen Physiol* **80,** 279–297.

Gruen M, Prinz H & Gautel M (1999). cAPK-phosphorylation controls the interaction of the regulatory domain of cardiac myosin binding protein C with myosin-S2 in an on-off fashion. *FEBS Lett* **453,** 254–259.

Gupta MK, Gulick J, James J, Osinska H, Lorenz JN & Robbins J (2013). Functional dissection of myosin binding protein C phosphorylation. *J Mol Cell Cardiol* **64,** 39–50.

Hanft LM, Korte FS & McDonald KS (2008). Cardiac function and modulation of sarcomeric function by length. *Cardiovasc Res* **77,** 627–636.

Hanft LM & McDonald KS (2009). Sarcomere length dependence of power output is increased after PKA treatment in rat cardiac myocytes. *Am J Physiol Heart Circ Physiol* **296**, H1524–1531.

Hanft LM & McDonald KS (2010). Length dependence of force generation exhibit similarities between rat cardiac myocytes and skeletal muscle fibres. *J Physiol* **588**, 2891–2903.

Hartzell HC & Titus L (1982). Effects of cholinergic and adrenergic agonists on phosphorylation of a 165,000-dalton myofibrillar protein in intact cardiac muscle. *J Biol Chem* **257,** 2111–2120.

Hofmann PA & Lange JH 3rd (1994). Effects of phosphorylation of troponin I and C protein on isometric tension and velocity of unloaded shortening in skinned single cardiac myocytes from rats. *Circ Res* **74,** 718–726.

Howarth JW, Ramisetti S, Nolan K, Sadayappan S & Rosevear PR (2012). Structural insight into unique cardiac myosin-binding protein-C motif: a partially folded domain. *J Biol Chem* **287,** 8254–8262.

Jacques AM, Copeland O, Messer AE, Gallon CE, King K, McKenna WJ, Tsang VT & Marston SB (2008). Myosin binding protein C phosphorylation in normal, hypertrophic and failing human heart muscle. *J Mol Cell Cardiol* **45,** 209–216.

Janssen PM & de Tombe PP (1997). Protein kinase A does not alter unloaded velocity of sarcomere shortening in skinned rat cardiac trabeculae. *Am J Physiol* **273,** H2415–2422.

Jeffries CM, Whitten AE, Harris SP & Trewhella J (2008). Small-Angle X-ray Scattering Reveals the N-Terminal Domain Organization of Cardiac Myosin Binding Protein C. *J Mol Biol* **377,** 1186–1199.

Jia W, Shaffer JF, Harris SP & Leary JA (2010). Identification of novel protein kinase A phosphorylation sites in the M-domain of human and murine cardiac myosin binding protein-C using mass spectrometry analysis. *J Proteome Res* **9,** 1843–1853.

Kuster DWD, Sequeira V, Najafi A, Boontje NM, Wijnker PJM, Witjas-Paalberends ER, Marston SB, Dos Remedios CG, Carrier L, Demmers JAA, Redwood C, Sadayappan S & van der Velden J (2013). GSK3β phosphorylates newly identified site in the proline-alanine-rich

29

region of cardiac myosin-binding protein C and alters cross-bridge cycling kinetics in human: short communication. *Circ Res* **112,** 633–639.

Layland J, Solaro RJ & Shah AM (2005). Regulation of cardiac contractile function by troponin I phosphorylation. *Cardiovasc Res* **66,** 12–21.

Mason DT, Braunwald E, Covell JW, Sonnenblick EH & Ross J (1971). Assessment of Cardiac Contractility The Relation Between the Rate of Pressure Rise and Ventricular Pressure During Isovolumic Systole. *Circulation* **44,** 47–58.

McDonald KS, Hanft LM, Domeier TL & Emter CA (2012). Length and PKA Dependence of Force Generation and Loaded Shortening in Porcine Cardiac Myocytes. *Biochem Res Int* **2012**, 371415.

Merkulov S, Chen X, Chandler MP & Stelzer JE (2012). In vivo cardiac myosin binding protein C gene transfer rescues myofilament contractile dysfunction in cardiac myosin binding protein C null mice. *Circ Heart Fail* **5,** 635–644.

Moss RL, Razumova M & Fitzsimons DP (2004). Myosin Crossbridge Activation of Cardiac Thin Filaments Implications for Myocardial Function in Health and Disease. *Circ Res* **94,** 1290–1300.

Nagayama T, Takimoto E, Sadayappan S, Mudd JO, Seidman JG, Robbins J & Kass DA (2007). Control of in vivo left ventricular [correction] contraction/relaxation kinetics by myosin binding protein C: protein kinase A phosphorylation dependent and independent regulation. *Circulation* **116,** 2399–2408.

Palmer BM, Sadayappan S, Wang Y, Weith AE, Previs MJ, Bekyarova T, Irving TC, Robbins J & Maughan DW (2011). Roles for cardiac MyBP-C in maintaining myofilament lattice rigidity and prolonging myosin cross-bridge lifetime. *Biophys J* **101,** 1661–1669.

Previs MJ, Beck Previs S, Gulick J, Robbins J & Warshaw DM (2012). Molecular mechanics of cardiac myosin-binding protein C in native thick filaments. *Science* **337,** 1215–1218.

Sadayappan S, Gulick J, Osinska H, Barefield D, Cuello F, Avkiran M, Lasko VM, Lorenz JN, Maillet M, Martin JL, Brown JH, Bers DM, Molkentin JD, James J & Robbins J (2011).

A critical function for Ser-282 in cardiac Myosin binding protein-C phosphorylation and cardiac function. *Circ Res* **109,** 141–150.

Sadayappan S, Gulick J, Osinska H, Martin LA, Hahn HS, Dorn GW, Klevitsky R, Seidman CE, Seidman JG & Robbins. J (2005). Cardiac Myosin Binding Protein-C Phosphorylation and Cardiac Function. *Circ Res* **97,** 1156–1163.

Shaffer JF, Kensler RW & Harris SP (2009). The myosin-binding protein C motif binds to F-actin in a phosphorylation-sensitive manner. *J Biol Chem* **284,** 12318–12327.

Stelzer JE, Fitzsimons DP & Moss RL (2006*a*). Ablation of Myosin-Binding Protein-C Accelerates Force Development in Mouse Myocardium. *Biophys J* **90,** 4119–4127.

Stelzer JE, Patel JR & Moss RL (2006*b*). Protein kinase A-mediated acceleration of the stretch activation response in murine skinned myocardium is eliminated by ablation of cMyBP-C. *Circ Res* **99,** 884–890.

Stelzer JE, Patel JR & Moss RL (2006*c*). Acceleration of stretch activation in murine myocardium due to phosphorylation of myosin regulatory light chain. *J Gen Physiol* **128,** 261–272.

Stelzer JE, Patel JR, Walker JW & Moss RL (2007). Differential roles of cardiac myosin-binding protein C and cardiac troponin I in the myofibrillar force responses to protein kinase A phosphorylation. *Circ Res* **101,** 503–511.

Tong CW, Stelzer JE, Greaser ML, Powers PA & Moss RL (2008). Acceleration of crossbridge kinetics by protein kinase A phosphorylation of cardiac myosin binding protein C modulates cardiac function. *Circ Res* **103,** 974–982.

Tong CW, Nair NA, Doersch KM, Liu Y & Rosas PC (2014). Cardiac myosin-binding protein-C is a critical mediator of diastolic function. *Pflüg Arch Eur J Physiol* **466**, 451–457.

Walker JS, Walker LA, Margulies K, Buttrick P & de Tombe P (2011). Protein kinase A changes calcium sensitivity but not crossbridge kinetics in human cardiac myofibrils. *Am J Physiol Heart Circ Physiol* **301,** H138–146.

Wang L, Ji X, Barefield D, Sadayappan S & Kawai M (2014). Phosphorylation of cMyBP-C Affects Contractile Mechanisms in a Site-specific Manner. *Biophys J* **106,** 1112–1122.

Weith AE, Previs MJ, Hoeprich GJ, Previs SB, Gulick J, Robbins J & Warshaw DM (2012). The extent of cardiac myosin binding protein-C phosphorylation modulates actomyosin function in a graded manner. *J Muscle Res Cell Motil* **33**, 449-459.

TABLES

Table 1: LV morphology and *in vivo* cardiac performance measured by echocardiography.

	NTG	TG^{WT}	TG^{S282A}
BW (g)	26.6±1.5	24.0±2.3	25.8±1.0
LV Mass/BW	3.8±0.2	4.1±0.3	4.3±0.2
HR (beats/min)	412±14	401±22	420±13
PWd (mm)	0.9±0.1	0.9±0.1	1.0±0.1
PWs (mm)	1.1±0.1	1.1±0.1	1.2±0.1
IVRT (msec)	19.8±1.6	21.3±1.5	21.9±1.6
FS (%)	36.0±2.3	33.9±2.2	32.1±1.7
EF (%)	72.6±2.5	71.1±2.1	68.5±2.0

BW: body weight; LV Mass/BW; ratio of LV and body weight; HR; heart rate; PWd: posterior wall thickness in diastole; PWs: posterior wall thickness in systole; IVRT: isovolumic relaxation time; FS: fractional shortening; EF: ejection fraction. Values are expressed as mean ± SEM from 8 mice per group.

Table 2: Left ventricular hemodynamic function measured by P-V loop analysis

Group	HR (beats/min)	ESP (mmHg)	EDP (mmHg)	dP/dt_{max} (mmHg/s)	τ (ms)
- DOB					
NTG	434 ± 11	97.0 ± 2.8	7.51 ± 0.35	$7,013 \pm 409$	9.15 ± 0.50
TG^{WT}	418 ± 6	100.8 ± 4.4	7.97 ± 1.22	$6,861 \pm 517$	10.08 ± 0.51
TG^{S282A}	447 ± 11	92.5 ± 1.5	7.62 ± 1.14	$6,064 \pm 144$	10.62 ± 0.36
+DOB					
NTG	509 ± 12*	93.7 ± 3.4	5.16 ± 0.57*	$12,132 \pm 298$*	7.60 ± 0.67*
TG^{WT}	509 ± 12*	99.8 ± 4.0	6.63 ± 1.07	$11,188 \pm 581$*	8.62 ± 0.32*
TG^{S282A}	545 ± 10*	93.3 ± 2.1	4.97 ± 0.68*	$8,993 \pm 421$*†	8.99 ± 0.42*

DOB: dobutamine; HR: heart rate; ESP: end systolic pressure; EDP: end diastolic pressure; dp/dt_{max}: maximum rate of pressure development; τ: time constant of pressure relaxation. Values are expressed as mean ± SEM. n = 6 for NTG, 9 for TG^{WT}, and 8 for TG^{S282A}. * Significantly different from the corresponding baseline group (without dobutamine treatment), $P < 0.05$. † Significantly different from TG^{WT}, $P < 0.05$.

Table 3: Steady-state mechanical properties of skinned myocardial fibers isolated from NTG and TG hearts

Group	F_{min} (mN/mm^2)	F_{max} (mN/mm^2)	n_H	pCa_{50}
- PKA				
NTG	0.61±0.25	22.13±1.73	4.10±0.45	5.82±0.02
TG^{WT}	0.69±0.20	21.74±2.02	4.27±0.56	5.81±0.02
TG^{S282A}	0.64±0.21	21.41±1.92	4.34±0.66	5.82±0.02
+ PKA				
NTG	0.47±0.20	21.31±2.12	3.87±0.47	5.71±0.02[*]
TG^{WT}	0.52±0.17	20.88±1.71	4.11±0.50	5.70±0.02[*]
TG^{S282A}	0.51±0.19	20.47±1.84	3.79±0.63	5.73±0.03[*]

F_{min}: Ca^{2+}-independent force at pCa 9.0; F_{max}: maximal Ca^{2+}-activated force at pCa 4.5; n_H: Hill coefficient of the force-pCa relationship; pCa_{50}: pCa required for half-maximal force generation. Values are expressed as mean ± SEM, from 8 skinned fibers per group. * Significantly different from the corresponding non PKA-treated group, $P < 0.05$.

Table 4: Dynamic stretch-induced responses of skinned myocardial fibers isolated from NTG and TG hearts

Group	k_{df} (s^{-1})	k_{rel} (s^{-1})	P$_1$	P$_2$	P$_3$	P$_{df}$
- PKA						
NTG	10.07±0.32	442±30	0.588±0.029	0.030±0.004*	0.199±0.016	0.169±0.019
TG^{WT}	10.32±0.37	466±29	0.602±0.025	0.034±0.009*	0.191±0.024	0.157±0.022
TG^{S282A}	9.63±0.34	479±26	0.577±0.027	0.042±0.008*	0.203±0.027	0.161±0.024
+ PKA						
NTG	15.51±0.42*	761±46*	0.498±0.024*	-0.057±0.018*	0.194±0.021	0.251±0.024*
TG^{WT}	15.97±0.45*	748±52*	0.495±0.028*	-0.040±0.016*	0.205±0.028	0.245±0.026*
TG^{S282A}	13.01±0.41*†	717±40*	0.480±0.024*	-0.042±0.013*	0.214±0.030	0.256±0.027*

k_{df}: the rate constant of force development during stretch activation; k_{rel}: the rate constant of force decay during stretch activation; P$_1$: the peak force attained following a rapid stretch; P$_2$: the difference between pre-stretch steady-state force to the minimum force value at the end of phase 2 of stretch-activation protocol; P$_3$: the difference between pre-stretch steady-state force to the peak value of delayed force of stretch-activation protocol; P$_{df}$: the difference between P$_3$ and P$_2$. Values are expressed as means ± SEM, from 12 skinned fibers and 4 hearts per group. The comparisons were made at equivalent levels of activation, ~50% of maximal activation following a 2% stretch of initial muscle length. * Significantly different from the corresponding non PKA-treated group, $P < 0.05$. † Significantly different from TG^{WT}, $P < 0.05$.

FIGURE 1: Transgenic cMyBP-C expression and phosphorylation. **(A)** cMyBP-C is composed of eight Ig (oval shaped) and three FnIII (rectangle shaped) domains labeled C0 (N-terminus) through C10 (C-terminus) and has a conserved M-domain linker between C1 and C2 domains. The M-domain contains three serine residues (Ser273, Ser282, and Ser302, underlined) in the WT sequence that are targets for PKA phosphorylation. The substitution used to prevent phosphorylation of Ser282 in S282A TG protein is shown. Ig, immunoglobulin-like; FnIII, fibronectin type III. **(B)** Western blots of NTG and TG^{S282A} samples were probed with antibodies specific for phosphorylation of Ser273, Ser282, or Ser302, total cMyBP-C, myc tag, or HSC70. Western blot with an antibody to myc tag shows that a band corresponding to cMyBP-C with S282A was only detected in TG^{S282A} samples. **(C)** NTG and TG^{S282A} samples were stained with coomassie blue to determine the relative protein incorporation into the sarcomere. **(D)** The band intensities corresponding to protein expression were normalized to actin content to determine the relative protein expression. Values are expressed as mean ± SEM, from 6 hearts per group.
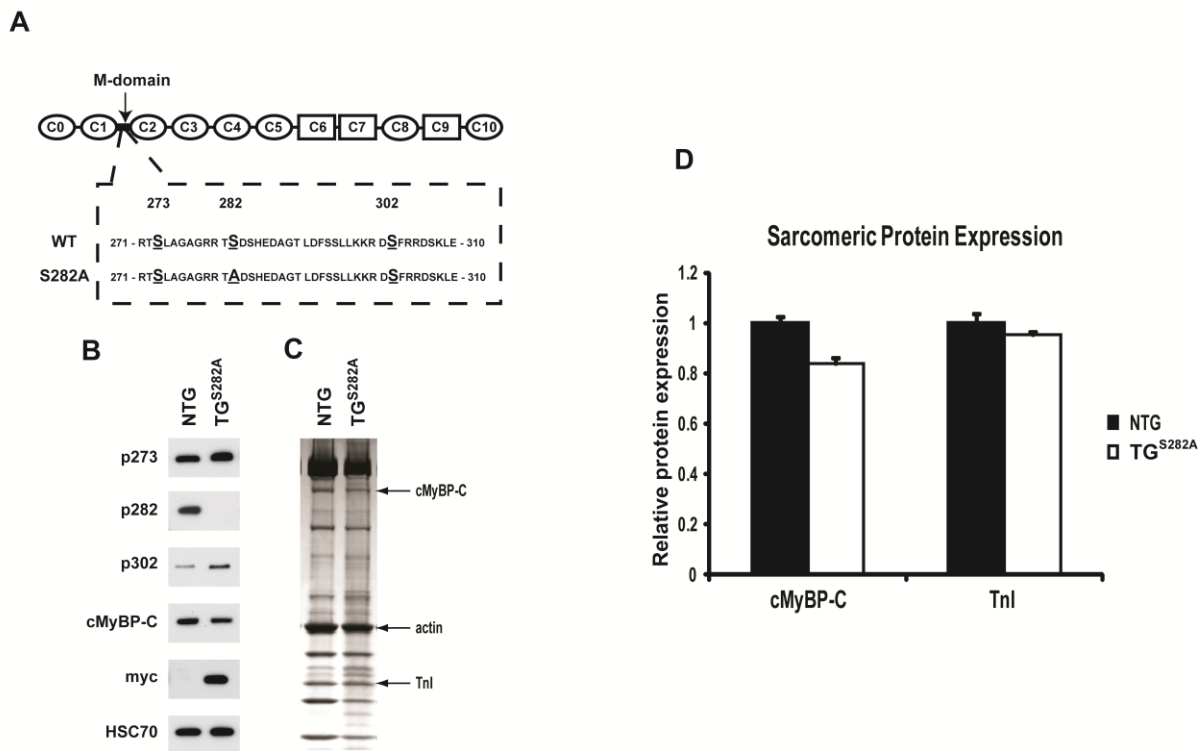
Figure 1

FIGURE 2: Determination of PKA-mediated phosphorylation of cMyBP-C and other sarcomeric proteins. **(A)** Myofibrils isolated from NTG, TG^{WT}, and TG^{S282A} hearts were treated with PKA and the phosphorylation of Ser273, 282, and 302 was assessed by Western Blot. Band intensity of the phosphorylated signal for each residue in non-PKA treated (-PKA, left) and PKA treated (+PKA, right) samples was normalized to total cMyBP-C expression. HSC70 was used to verify equal sample loading. **(B)** Relative protein phosphorylation (phosphorylated signal/total cMyBP-C) was calculated for each residue and is expressed as a % of PKA-treated TG^{WT} values for that residue. (C) Representative Western Blot showing the rate of PKA-mediated Ser273 and Ser302 phosphorylation. Samples were taken before the addition of PKA (0min) and every 15 minutes after the addition of PKA. No differences in the rate of Ser273 and Ser302 phosphorylation were observed between TG^{WT} and TG^{S282A} samples. Representative gels shown are stained by Pro-Q stain for protein phosphorylation **(D)** and coomassie for total protein **(E)**. cMyBP-C, TnT, TnI, and RLC are labeled in each image, and the same gel is shown in panels A and B. **(F)** The intensities of the phospho-bands normalized to total protein (i.e., phosphorylated TnI/total TnI) are expressed as a % of PKA-treated TG^{WT} phosphorylation. Values are expressed as mean ± SEM, from 4 NTG hearts, and 8 TG^{WT} and 8 TG^{S282A} hearts. * Significantly different from non-PKA treated samples from the same line, $P < 0.05$; † Significantly different from the non PKA-treated TG^{WT}, $P < 0.05$.
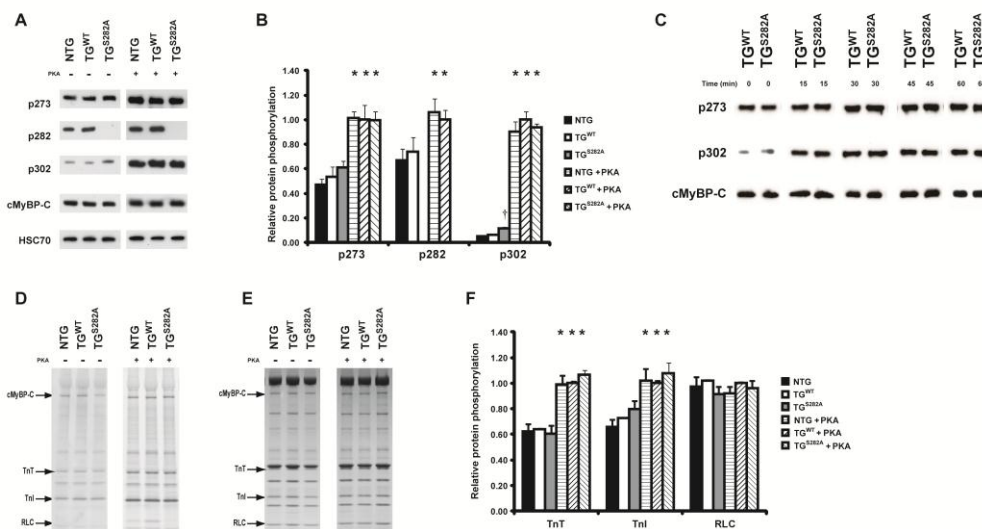
Figure 2

FIGURE 3: Analysis of cardiac morphology. (**A**) Representative NTG, TG^{WT}, and TG^{S282A} formalin fixed hearts showing overall cardiac morphology, with the left ventricle indicated by an arrow. The scale bar is 1mm. Representative cross sections of NTG, TG^{WT}, and TG^{S282A} hearts from the mid-LV were stained with H&E and imaged at 100X magnification, with digital zoom used to reduce the image in **B**, to examine the cardiac morphology. The scale bars in (**B**) are 1mm and in (**C**) are 50µm.
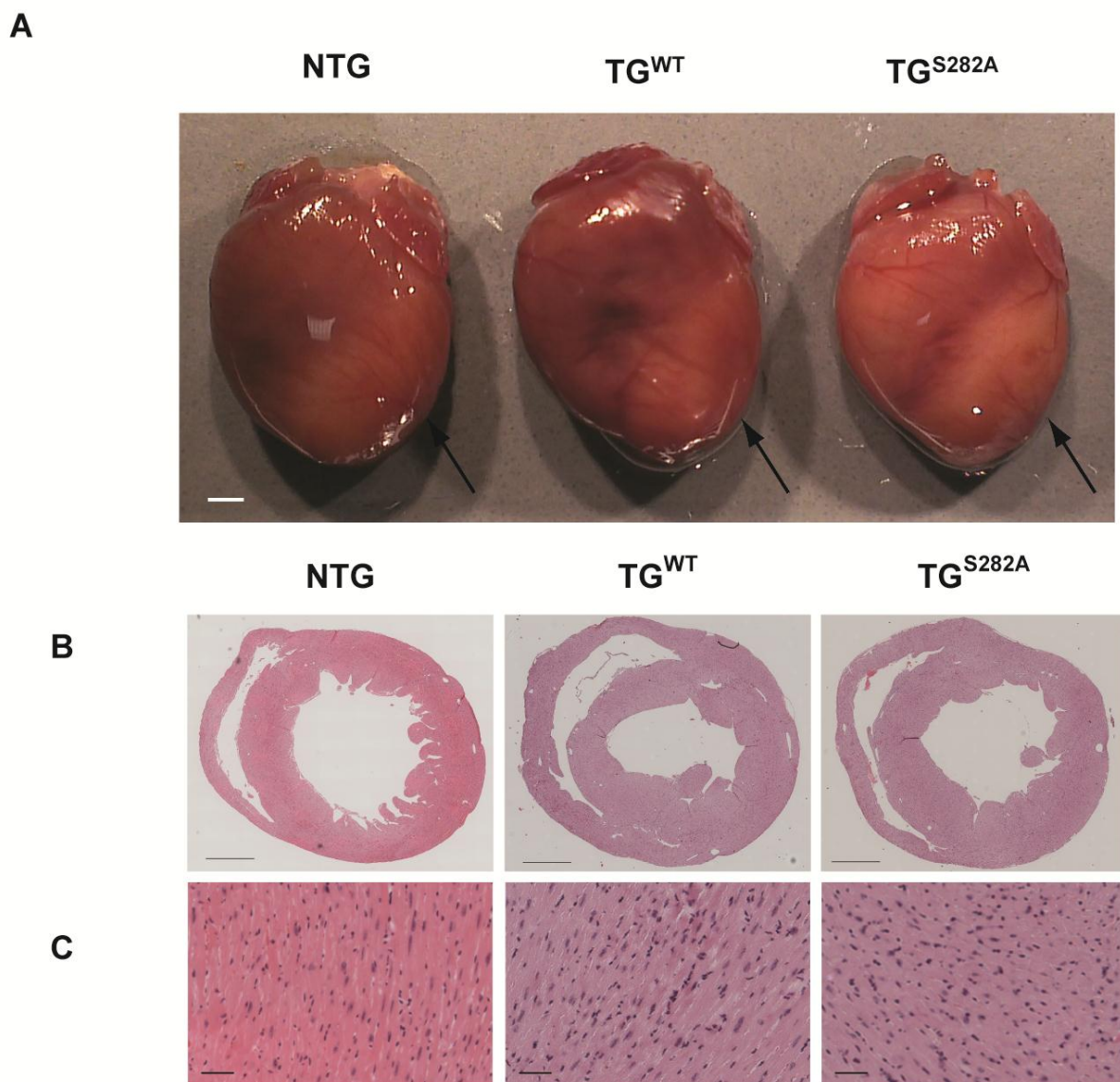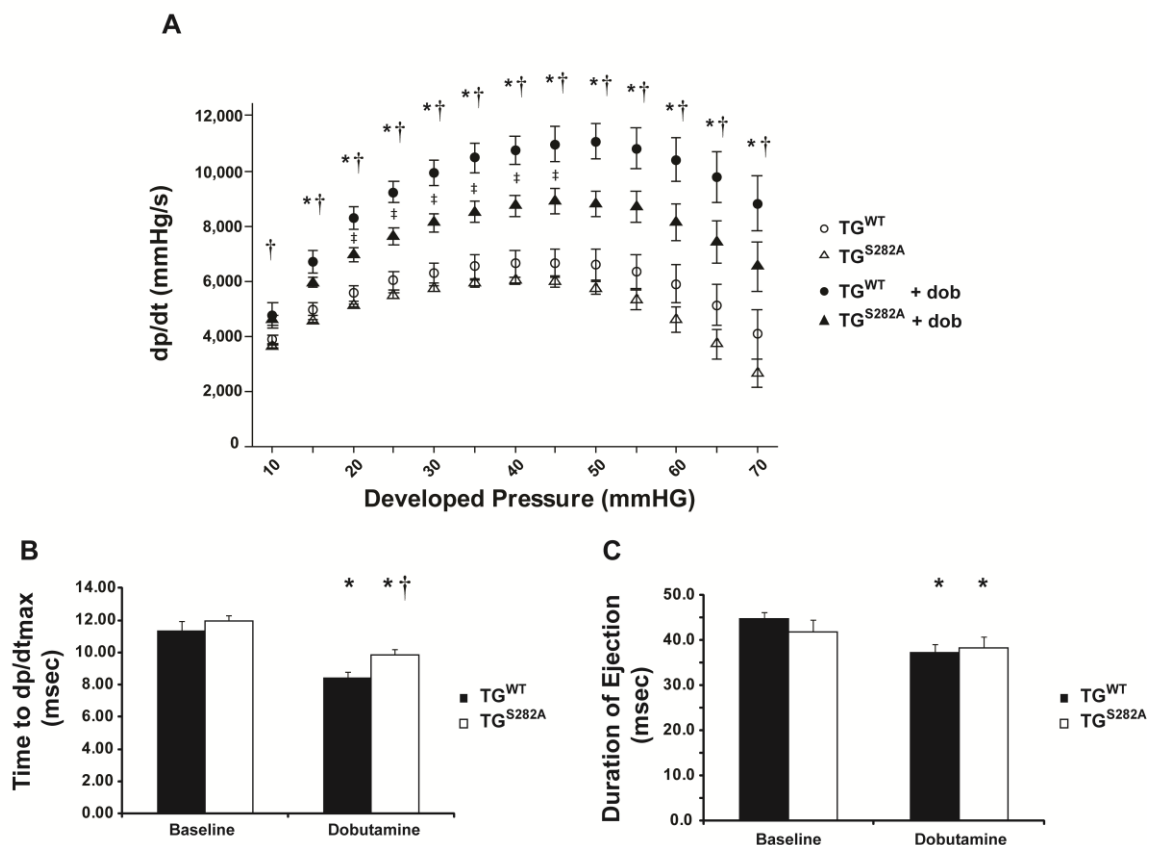
Figure 3

FIGURE 4: Analysis of the rate of pressure development. (A) The rate of pressure development (dp/dt) was measured over a range of developed pressures during isovolumic contraction. End diastolic pressure was subtracted from instantaneous ventricular pressure to yield developed pressure. Dobutamine significantly increased dp/dt in both TG^{WT} and TG^{S282A}; however, the shift was blunted in TG^{S282A} hearts. * TG^{WT} + dobutamine significantly different from the TG^{WT} baseline (without dobutamine treatment), $P < 0.05$; † TG^{S282A} + dobutamine significantly different from the TG^{S282A} baseline (without dobutamine treatment), $P < 0.05$; ‡ TG^{S282A} + dobutamine significantly different from TG^{WT} + dobutamine, $P < 0.05$. (**B**) The time taken to reach dp/dt$_{max}$ t_d measured from end-diastole. Dobutamine shortened t_d in both TG^{WT} and TG^{S282A}, but TG^{S282A} hearts took significantly longer time to reach dp/dt$_{max}$. (**C**) The duration of ejection was unaltered by TG S282A expression, as TG^{S282A} hearts showed no differences either at baseline or after dobutamine compared to TG^{WT} hearts. For (**B**) and (**C**): * Significantly different from the corresponding baseline (non-dobutamine treated) group, $P < 0.05$; † Significantly different from the dobutamine-treated TG^{WT} group, $P < 0.05$.

Figure 4

Accepted Article

41

FIGURE 5: Effect of PKA-mediated phosphorylation on k_{tr} at half-maximal Ca^{2+} activation. (A) k_{tr} was measured at 50% of maximal Ca^{2+} activation, and shows that PKA treatment (open bars) accelerated k_{tr} in NTG (lane 1), TG^{WT} (lane 2) TG^{S282A} (lane 3) fibers when compared to the corresponding non PKA-treated fibers (solid bars). Values are expressed as mean ± SEM, from 12 skinned fibers and 4 hearts per group. * Significantly different from the corresponding baseline (non-PKA treated) group, $P < 0.05$; † Significantly different from the PKA-treated TG^{WT} group, $P < 0.05$. (B) Representative force traces following a mechanical slack and restretch protocol demonstrating PKA-mediated acceleration of the rate of force redevelopment (k_{tr}) in TG^{S282A} skinned myocardium. Fibers were activated in a pCa solution that produced ~50% of maximal force prior to (black trace) and following PKA treatment (grey trace).
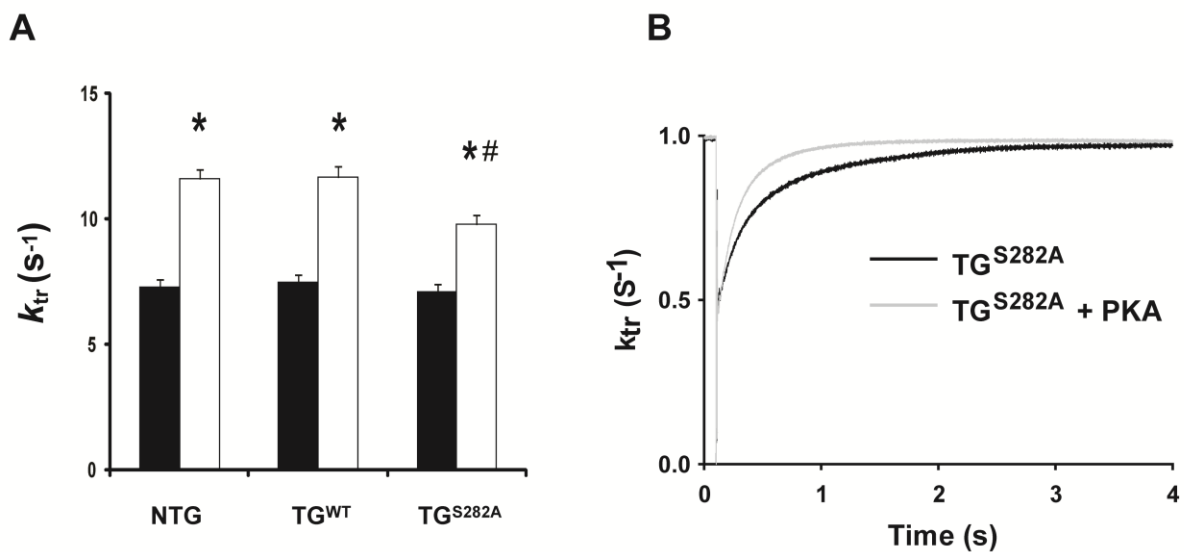
Figure 5

FIGURE 6: Effects of PKA treatment on the stretch activation responses of TG^{S282A}
myocardium. Force transients following a stretch of 2% of muscle length were recorded at
$[Ca^{2+}]$ yielding a pre-stretch isometric force of ~50% maximal prior to (black trace) and
following PKA treatment (grey trace) in TG^{S282A} skinned myocardium. These representative
transients are normalized to pre-stretch isometric force corresponding to the force base-line,
which is arbitrarily set at zero, and demonstrate that PKA treatment significantly accelerated
the overall stretch-activation response in TG^{S282A} skinned myocardium. The stretch activation
parameters that were investigated are represented in the trace and are described in detail in
the text.

Figure 6